Articles

Synthesis and Stabilization of Stibine for Low-Temperature Chemical Vapor Deposition of Carbon-Free Antimony Films

Michael A. Todd, Gautam Bandari, and Thomas H. Baum*

Advanced Technology Materials, Inc., Advanced Delivery and Chemical Systems Division, 7 Commerce Drive, Danbury, Connecticut 06810

Received March 3, 1998. Revised Manuscript Received December 22, 1998

Antimony trihydride(stibine), SbH_3, and antimony trideuteride, SbD_3, were synthesized in high yields via a unique nonaqueous synthetic route. A study comparing the relative thermal stability of SbD_3 with that of SbH_3 was performed. Deuterated stibine displays significantly greater thermal stability than its hydride analogue due to isotopic stabilization and can be stored at room temperature for weeks with minimal decomposition. The thermal decomposition of SbD_3 was performed at 300 °C in a horizontal, hot-wall chemical vapor deposition (CVD) reactor. Decomposition efficiencies approaching 50% were achieved when SbD_3 was delivered with H_2 as a carrier gas. As this research demonstrates, deuterated stibine is an improved CVD source due to its gaseous nature, compositional simplicity, lack of Sb−C bonds, enhanced thermal stability, and ability to deposit Sb films at very low temperatures.

Introduction

Sophisticated microelectronic components and device heterostructures are driving the development of chemical vapor deposition (CVD) precursors that exhibit useful volatility and the ability to deposit high-purity films at low temperatures. Currently, many III−V devices based upon strained layer superlattices and multiple quantum wells (MQW) are fabricated by molecular beam epitaxy (MBE). MBE is relatively slow and expensive when compared to alternate thin-film growth techniques used for microelectronics. Although CVD offers a low-cost, high throughput approach to device manufacturing, a lack of suitable, low-temperature CVD precursors has hindered its widespread applicability.[1,2] This is particularly true for Sb-based heterostructures that display important optoelectronic and electronic properties, including InSb,[3] InGaSb,[4] InAsSb,[5] GaAlSb,[6] and InSbBi.[7] Volatile and thermally stable Sb precursors would facilitate the chemical vapor deposition of antimonide thin films, as required for the large scale, controlled production of Sb-based lasers, detectors, and sensors.[8]

Antimonide materials are attractive for commercial infrared optoelectronic applications. The compositional variety and stoichiometry of III−V compound semiconductors allows for nearly complete coverage of the infrared spectrum. Band gaps ranging from 2.5 eV in AlP to 0.2 eV in InSb can be achieved by forming strained thin films with the proper elemental and stoichiometric compositions. Materials of greatest interest include InSbBi and InAs−SbBi[9] for long wavelength (8−12 μm) infrared detectors, InAsSb[10] and InGaSb[11] for mid-infrared absorbers in military applications, and $InSb/In_{1-x}Al_xSb$[12] light-emitting diodes (LEDs) for mid-infrared chemical sensor applications. Many of these materials, however, are metastable compositions that necessitate low processing temperatures. Further, the inherent physical properties of Ga, Sb, and In necessitate low processing temperatures to alleviate interdiffusion, melting, and re-evaporation (i.e., InSb melts

(1) Lin, C. H.; Murry, S. J.; Zhang , D.; Chang, P. C.; Zhou, Y.; Pei, S. S.; Malin, J. I.; Felix, C. L.; Meyer, J. R.; Hoffman, C. A..; Pinto, J. F. *J. Cryst.* Growth **1997**, *175*, 955.
(2) Stauf, G. T.; Gaskill, D. K.; Bottka, N..; Gedridge, Jr., R. W. *Appl. Phys. Lett.* **1991**, *58* (12), 1311.
(3) Gaskill, D. K.; Stauf, G. T..; Bottka, N. *Appl. Phys. Lett.* **1991**, *58* (17), 1905.
(4) Lin, C. H.; Yang, R. Q.; Zhang, D.; Murry, S. J.; Pei, S. S.; Allerma, A. A..; Kurtz, S. R. *Electron Lett.* **1997**, *33*, 598.
(5) Kim, J. D.; Wu, D.; Wojkowski, J.; Piotrowski, J.; Xu, J..; Razeghi, M. *Appl. Phys. Lett.* **1996**, *68*, 99.
(6) Bocchi, C.; Bosacchi, A.; Franchi, S.; Gennari, S.; Magnanini, R..; Drigo, A. V. *Appl. Phys. Lett.* **1997**, *71* (11), 1549.
(7) Lee, J. J.; Kim, J. D..; Razeghi, M. *Appl. Phys. Lett.* **1997**, *70*(24), 3266.
(8) Yang, J.; Heremans, J.; Partin, D. L.; Thrush, C. M..; Naik, R. *J. Appl. Phys.* **1998**, *83* (4), 2041.
(9) Stauf, G. T.; Gaskill, D. K.; Bottka, N..; Gedridge, C. W., Jr. *Mater. Res. Soc. Symp. Proc.* Vol. **1991**, *216*, 239.
(10) Lane, B.; Wu, D.; Rybaltowski, A.; Yi, H.; Diaz, J..; Razeghi, M. *Appl. Phys. Lett.* **1997**, *70*, 443.
(11) Boggess, T. F.; McCahon, S. W.; Anson, S. T.; Olesberg, J. T.; Flatte, M. E.; Chow, D. H.; Hasenberg, T. C.; Grein, C. H. Electronic Materials Conference, Santa Barbara, CA, 1996.
(12) Kurtz, S. R.; Biefeld, R. M.; Allerman, A. A..; Hjalmarson, H. J. Electronic Materials Conference, Santa Barbara, CA, 1996.

10.1021/cm980121m CCC: $18.00
Published on Web 02/02/1999

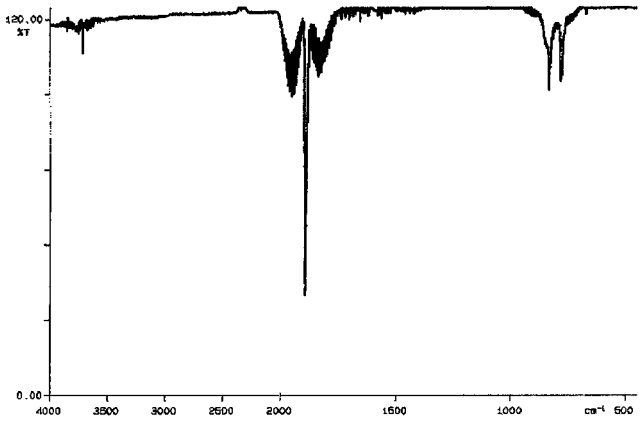

Figure 1. FTIR spectrum of proteostibine, SbH_3, showing strong Sb−H stretching centered at 1891, 1944, and 1830 cm^{-1}. Also visible is weak Sb−H bending, observed at 828 and 782 cm^{-1}.

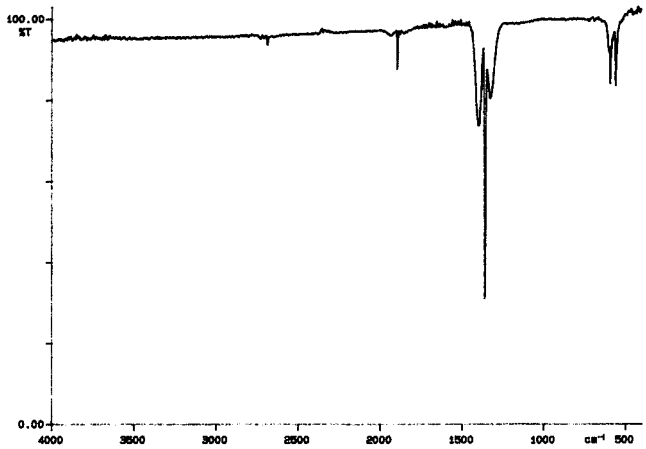

Figure 2. FTIR spectrum of deuterostibine, SbD_3, showing strong Sb-D stretching centered at 1356, 1399, and 1320 cm^{-1}. The Sb-D stretching and bending modes are shifted relative to SbH_3. The reduced vibrational frequencies result from substitution of D for H, in accordance with Hooke's law, and this isotope effect is responsible for the enhanced thermal stability observed in SbD_3.

at 525 °C).[13] Unfortunately, current Sb CVD sources, such as trimethyl antimony, require processing temperatures in excess of 420 °C to achieve useful film growth rates.

In this work, we describe a nonaqueous synthetic route and thermal decomposition of deuterated stibine, SbD_3, a precursor that offers carbon-free Sb deposition at substrate temperatures below 300 °C. Relative to its hydride analogue, SbD_3 exhibits enhanced thermal stability at room temperature and can be stored for prolonged periods of time without significant decomposition, at pressures below 10 Torr. As demonstrated by this research, an isotope effect can be used to stabilize metal hydride sources for the low-temperature, chemical vapor deposition of thin films.

Results and Discussion

Precursor Synthesis. Stibine, SbH_3, is a gas (mp −88 °C, bp −18 °C) that is reportedly unstable even at temperatures as low as −65 °C.[14] SbH_3 (**1**) was synthesized in high yield via a new synthetic reaction of antimony(III) chloride and lithium aluminum hydride in tetraethylene glycol dimethyl ether ("tetraglyme") solvent at −30 °C, as depicted in eq 1.

$$SbCl_3 + LiAlH_4 \rightarrow SbH_3(g) \quad (85\%) \qquad (1)$$

Other reductants, such as $NaBH_4$ and LiH, can also be employed for the synthesis of stibine, but $LiAlH_4$ was found to give the highest yields. The stibine generated from this reaction was trapped in a cold trap maintained at −130 °C. The use of a high-boiling coordinating solvent, such as tetraglyme (T_b = 275 °C), is particularly useful in separating stibine from the reaction mixture. The synthesis of SbH_3 was confirmed by comparison of its vapor-phase FTIR spectrum with that reported in the literature.[15] The gas-phase FTIR spectrum of stibine obtained at 20 Torr pressure is shown in Figure 1. The strongest absorption band, centered at 1891 cm^{-1}, is due to the Sb−H stretching mode. The Sb−H bending modes are clearly visible at 828 and 782 cm^{-1}. The only other distinguishing feature in the spectrum arises from a stretching vibrational overtone centered at about 3720 cm^{-1}.

Deuterated stibine, SbD_3 (**2**), was synthesized by replacing $LiAlH_4$ with $LiAlD_4$ in the synthetic procedure described above. Once again, the use of other deuterated reducing agents, such as $NaBD_4$ and LiD, lowered the yields of SbD_3. Characterization was accomplished by gas-phase FTIR spectroscopy and by comparison to the spectrum obtained for SbH_3. A typical SbD_3 spectrum is presented in Figure 2. The most striking feature of the spectrum is its similarity to that of SbH_3 in terms of the observed stretching and bending modes. As expected, and in accordance with Hooke's Law, spectral shifts are observed in SbD_3 due to the increased mass of deuterium relative to hydrogen. The Sb−D stretch is observed at 1356 cm^{-1} and corresponds to an isotopic shift ($\Delta\nu$) of over 500 cm^{-1} relative to the energy of the Sb−H stretch. The bending modes are observed at 590 and 558 cm^{-1}; the overtone vibrational mode is observed at 2683 cm^{-1}.

Deuterium substitution for the hydrogen atom offers a unique opportunity to thermally stabilize antimony hydrides including stibine. This phenomenon, commonly referred to as the primary isotope effect, is due to the lower zero-point energy of deuterated stibine compared to the proteostibine. As a result of the lowering of the ground state energy, the deuterated compound is more thermally stable. The maximum theoretical value of k_H/k_D is approximately 6.5 for reactions involving cleavage of C−H and C−D bonds. When hydrogen atoms are bound to heavier elements, such as transition metals, the kinetic isotope effect may be estimated by a first approximation using an infrared vibrational stretch; in this specific case, the Sb−H and Sb-D stretches can be compared. Assuming that the loss of the zero-point energy is the major contributor to the isotope effect in these materials, then we may calculate the k_H/k_D after estimation of the activation energy differences.[16] Using this methodology, we calculated the k_H/k_D ratio to be 3.7 at 21 °C based upon the measured Sb−H and Sb-D

(13) Sigiura, O.; Kameda, H.; Shina, K.; Matsumara, M. *J. Electron. Mater.* **1988**, *17* (1), 11.
(14) Olschewski, K. *Berichte Deutschen Chemischen Gesellshaft* **1901**, *34*, 3592.
(15) Halonen, H.; Halonen, L.; Burger, H..; Moritz, P. *J. Chem. Phys.* **1991**, *95*(10), 7099.

stretches, at 1891 and 1356 cm^{-1}, respectively. Although quantum mechanical tunneling could provide a facile mechanism for the decomposition of stibine, the lowering of the ground state energy, a result of the increased mass of the deuterium isotope, effectively increases the energy barrier to activation. Thus, the isotope effect can be exploited, as demonstrated in this study, to stabilize stibine as a CVD precursor.

Thermal Stability Comparison. The thermal stability of SbD_3 was compared to that of SbH_3 by storing equivalent amounts of each gas in separate glass containers of identical volume. By monitoring the total pressure with a capacitance manometer, it was possible to observe the decomposition of the stibines and the associated pressure increase arising from the evolution of H_2 or D_2 gas as a function of time. In a kinetic study that used an initial pressure (P_o) of 10 Torr, of either SbH_3 or SbD_3 in separate 250 mL glass storage flasks, the improved stability of SbD_3 relative to SbH_3 at 23 °C was clearly demonstrated. The total pressure in the SbH_3 container was observed to increase with time, while the SbD_3 container exhibited no pressure change with time. After 3 days of storage at 23 °C, all of the SbH_3 was decomposed. This was confirmed by the visual observation of an antimony metal film on the surface of the glass container, the presence of a noncondensable gas at −196 °C (i.e., H_2), and the absence of Sb−H stretching in the gas-phase FTIR spectrum of the residual gas. Upon monitoring SbD_3, it was not possible to observe any decomposition even after 1 week of storage at 23 °C, as confirmed by monitoring the FTIR of the Sb−D stretch. Preliminary studies conducted in glass indicate that the critical pressure for SbD_3 decomposition lies between 10 and 20 Torr. Slow, but continuous, decomposition was observed over a period of days for SbD_3 stored at pressures above 20 Torr. Rapid and complete decomposition was observed for storage pressures of 300 Torr or greater. Thus, concentration effects are critical toward the thermal decomposition rates and long-term storage of this precursor.

At first glance, the low critical pressure of SbD_3 at room temperature would appear to limit storage and the commercial utility of this precursor. However, by employing a newly developed adsorbant technology,[17] it was possible to store SbD_3 on adsorbents at weight loadings in excess of 30 wt %. Under these conditions, multiple gram quantities of SbD_3 have been stored at 23 °C for periods of up to 2 weeks with virtually no decomposition. Furthermore, after room-temperature storage for 2 weeks, it was possible to recover >70% of the adsorbed SbD_3 by vacuum removal and condensation into a trap maintained at −196 °C.

A comparison of the surface-adsorbed stability of SbD_3 relative to SbH_3 also revealed that SbD_3 is the more stable species. The storage of SbD_3 and SbH_3 on 1 mm diameter, spherically shaped carbon adsorbents, at weight loadings of 14.1% and 13.6%, respectively, was studied under identical conditions. The total pressure

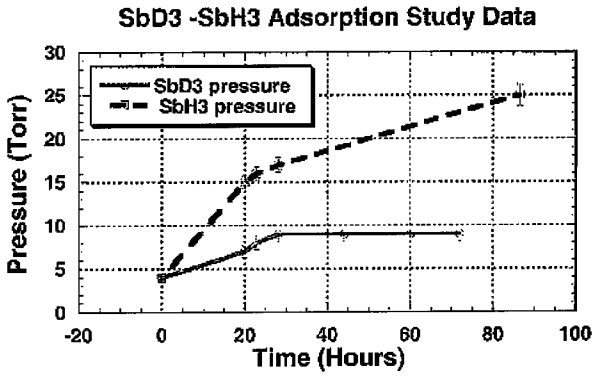

Figure 3. Total pressure measured over adsorbed SbH_3 and SbD_3 as a function of time for weight loadings of 13.6% and 14.1%, respectively. The pressure increase results from the formation of hydrogen (deuterium) gas as the stibine slowly decomposes. The initial pressure rise is indicative of surface-related decomposition, upon adsorption on the adsorbent carbon and is 3.2 times faster for SbH_3 relative to SbD_3. The plot clearly shows that deuterostibine is considerably more stable than the proteostibine.

over the adsorbed gases was measured as a function of time to observe pressure changes related to decomposition, as shown in Figure 3. Relative comparison of the initial slopes can be used to calculate the ratio of k_H/k_D; the decomposition rate for proteostibine is 3.2 times faster than that of deuterostibine, under identical conditions, in good agreement with the theoretically calculated isotope effect of 3.7. The shape of the curve suggests a bimodal decomposition mechanism for adsorbed SbH_3. We believe this bimodal decomposition indicates two mechanisms for thermal decomposition: one resulting from interaction with the solid adsorbent surface and one arising from inherent thermal decomposition. In the case of SbD_3, no decomposition is noted after the initial reaction with the carbon adsorbent surface. The enhanced stability of SbD_3 is demonstrated by a lower rate of pressure increase after carbon surface adsorption and by a much smaller total pressure increase with time. Further, gas-phase FTIR spectroscopy confirmed that SbD_3 was still present, after removal from the carbon adsorbent. The ability to store and recover large amounts of SbD_3, using adsorbent technology, demonstrates the viability of this precursor for the low-temperature CVD of carbon-free antimony films.

Film Deposition. Compound **2** was thermally decomposed in a horizontal, hot-walled, 1.5 in. diameter, low-pressure CVD reactor. The precursor was introduced both neat and in diluted mixtures with H_2 to yield films of antimony at temperatures as low as 200 °C. Films were deposited onto Pyrex, quartz, (100) Si and Pt overcoated (100) Si substrates. Typical depositions lasted 15 min to 1 h and resulted in films containing antimony with thicknesses ranging from 2500 Å to 10 000 Å. This corresponds to an average growth rate approaching 170 Å/min. Good adhesion was observed on Pt/Si, but the films were easily removed from Si, SiO_2, and Pyrex substrates. Films of up to 1 μm thick delaminated from all substrates, except for the Pt/Si substrate. The excellent adhesion observed for Pt/Si substrates is believed to be the result of the formation of antimony−platinum alloys. The XRD pattern of such a film (Figure 4) matches that of stumpflite, Pt_3Sb_2, an

(16) Lowry, T. H.; Richardson, K. S. *Mechanism and Theory in Organic Chemistry*, 3rd ed.; Harper and Row Publishers: New York, 1987; pp 232−238. Bigeleisen, J.; Goeppert Mayer, M. *J. Chem. Phys.* **1947**, *15* (5), 261.

(17) McManus, J. V.; Edwards, D.; Olander, W. K.; Kirk, R.; Romig, T.; Shi, J. *1996 11th International Conference on Ion Implantation Technology Proceedings*, 1997, p 804.

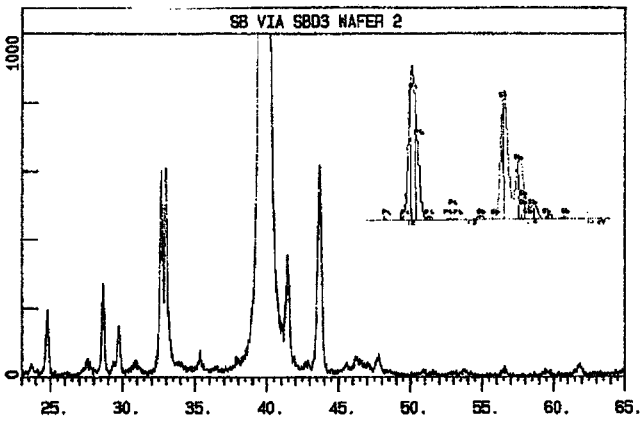

Figure 4. X-ray diffraction pattern of a 5000 Å film of Sb deposited using SbD_3 diluted in H_2 (1:40) at 300 °C. The pattern matches that of an alloy of Pt and Sb, stumpflite, Pt_2Sb_3; Pt; Sb; and a small amount of Sb_2O_3, believed to result from environmental exposure. The EDX spectrum (inset) reveals the presence of Sb and Pt, but not the small amount of O_2 observed in the XRD pattern.

alloy of Pt and Sb, and also shows overlap with Sb_2O_3. The EDX analysis shows only Pt and Sb within the film, indicating that the oxygen visible by XRD is probably a surface layer, formed by environmental exposure of the films after deposition (inset in Figure 4). AFM topographical analysis reveals very rough surfaces and the presence of pinholes within the films. EDX analysis of the pinholes revealed that they occurred at points where no Pt is present on the Si wafer.

Utilizing a −196 °C cold trap, attempts to trap decomposition byproducts revealed the presence of a noncondensable gas (presumed to be D_2) and unreacted SbD_3. The amount of SbD_3 consumed during CVD at 300 °C was estimated by recovering the unreacted SbD_3 from a 1:40 mixture of SbD_3 in H_2. Our analysis indicates that SbD_3 conversion approached 50% efficiency under these processing conditions. This decomposition efficiency is unexpectedly high, relative to other CVD precursors and processes, and demonstrates the applicability of SbD_3 for the low-cost, low-temperature deposition of carbon-free antimony films.

Conclusion

We have demonstrated the low-temperature, carbon-free deposition of antimony using deuterium-stabilized stibine gas, SbD_3. EDX analysis demonstrates that the films contain low concentrations of oxygen and, as expected, no carbon. We have also shown that storage of SbD_3 on spherical carbon adsorbents results in a practical room-temperature storage and delivery scheme. Further work related to the deposition of III−V compound semiconductors is currently underway in order to demonstrate the utility of SbD_3 as a low-temperature precursor for CVD of antimony films.

Experimental Section

General Procedures. All synthetic work was performed in a nitrogen-filled glovebox (Vacuum Atmospheres Model HE-553-4) or under dry nitrogen using standard vacuum line and Schlenk techniques. Unless noted otherwise, all chemicals were used as received from the vendor. The FTIR spectra were collected on a Perkin-Elmer model 1650 spectrometer. Nuclear magnetic resonance spectra were recorded on a Varian Gemini 200 MHz spectrometer.

Gas synthesis and purification (by trap−trap distillation) was conducted using a double-manifold high-vacuum line equipped with an oil diffusion pump, capable of pumping down to 10^{-7} Torr. All traps and glassware utilized were trace metal cleaned using NH_4OH:H_2O_2 and HNO_3 cleaning steps, followed by concentrated HCl rinse and a flowing distilled deionized water rinse. All glassware was oven dried at 120 °C prior to use.

Thin Film Deposition. The thin films described in this work were deposited in a horizontal, resistively heated, hot-walled CVD reactor (1.5 in. diameter). The depositions were temperature-controlled using a Eurotherm model 847 temperature controller, and both reactant and carrier gases were introduced via mass flow controllers. A base pressure of 5×10^{-5} Torr was maintained prior to depositions using a liquid nitrogen trapped diffusion pump. Processing pressures were monitored via a 1000 Torr capacitance manometer and varied by changing the reactant and carrier gas flow rates. The condensable gases from the reactions were collected in a liquid nitrogen cold trap (−196 °C) and were analyzed using FTIR and, when possible, NMR.

Film Composition. The composition and morphology of the films deposited was investigated using X-ray diffraction (XRD), energy-dispersive X-ray analysis (EDX), scanning electron microscopy (SEM), and atomic force microscopy (AFM). Film thickness was determined using a profilometer (model Dektak IIA).

I. Synthesis of SbH_3 (1). An authentic sample of stibine was synthesized via the reported aqueous synthetic route[18] in a 44% yield. Two new, nonaqueous synthetic routes (Methods A and B), provide higher yields and are reported herein. **CAUTION**: stibine is a highly toxic gas and should be handled in a well-ventilated area with the utmost care.

Method A. A 500 mL flask was charged with a suspension of $NaBaH_4$ (0.43 g, 11 mmol) in 100 mL of tetraglyme and cooled to 0 °C. A solution of $SbCl_3$ (0.5 g, 2.2 mmol) in 50 mL of tetraglyme was prepared in a nitrogen-filled glovebox and then placed in an addition funnel. The reaction flask and the addition funnel were connected under flowing nitrogen, followed by degassing of the apparatus by exposure to vacuum. The reaction was then initiated by slowly adding the antimony solution to the cooled, stirred sodium borohydride suspension. The suspension was observed to turn black with the continued addition of the antimony solution; gas evolution was readily evidenced by bubbling. The volatiles produced during the reaction were continuously passed through traps maintained at −20, −130, and −196 °C. The −130 °C trap was found to contain stibine (0.17 g, 1.4 mmol, 62%). The −20 °C trap was employed to condense any tetraglyme, but at the reaction temperature of 0 °C, none was observed. The −196 °C trap was found to contain a very volatile species that was tentatively identified as B_2H_6. **CAUTION**: The reaction byproduct, diborane, is toxic and highly reactive and should be handled and disposed of with great care.

Method B. A 500 mL flask was charged with a suspension of purified $LiAlH_4$ (0.51 g, 13 mmol) in 100 mL of tetraglyme and cooled to −30 °C. A solution of $SbCl_3$ (0.5 g, 2.2 mmol) in 50 mL of tetraglyme was prepared in a nitrogen-filled glovebox and then placed in an addition funnel. The reaction flask and the addition funnel were connected using standard Schlenck techniques and then degassed. The reaction was initiated by slowly adding the antimony solution to the cooled, stirred lithium aluminum hydride suspension. With continuing addition of the antimony solution, the suspension was observed to turn black; gas evolution was visually observed by bubbling. The volatiles produced during the reaction were continuously passed through traps maintained at −20 and −196 °C. The −196 °C trap was found to contain stibine (0.19 g, 1.7 mmol, 77%). The −20 °C trap was employed to condense any

(18) Jolly, W. E.; Drake, J. E. *Inorg. Synth.***1958**, *7*, 34.

tetraglyme, but at the reaction temperature of −30 °C, none was observed.

Vapor-phase FTIR of SbH_3: 3720 cm^{-1} (w), 1939 cm^{-1} (m,br), 1891 cm^{-1} (vs), 1846 cm^{-1} (m,br), 1154 cm^{-1} (vw), 840 cm^{-1} (w,sh), 828 cm^{-1} (m), 782 cm^{-1} (m).

II. Synthesis of SbD_3 (2). An authentic sample of deuterostibine was synthesized using a modification of the reported procedure[18] employing deuterated reducing agents. Similarly, two new, nonaqueous synthetic routes were examined employing deuterated reducing agents as a modification to the above methods. **CAUTION:** SbD_3 is expected to exhibit similar toxicological properties to stibine and other antimony compounds; it should be treated as an extremely toxic gas.

Method A. A 500 mL flask was charged with a suspension of $NaBaD_4$ (0.50 g, 12 mmol) in 100 mL of tetraglyme and cooled to −30 °C. A solution of $SbCl_3$ (0.52 g, 2.3 mmol) in 50 mL of tetraglyme was prepared in a nitrogen-filled glovebox and then placed in an addition funnel. The reaction was conducted using a procedure identical to that described in method B above. The volatiles produced during the reaction were continuously passed through traps maintained at −20, −130, and −196 °C. The −130 °C trap was found to contain deuterostibine (0.19 g, 1.5 mmol, 65%). The −20 °C trap was employed to condense any tetraglyme, but at the reaction temperature of −30 °C, none was observed. The −196 °C trap was found to contain a very volatile species that is tentatively identified as B_2D_6. **CAUTION**: diborane is toxic, highly reactive, and pyrophoric. It should be handled and disposed of carefully.

Method B. A 500 mL flask was charged with a suspension of purified $LiAlD_4$ (0.46 g, 11 mmol) in 100 mL of tetraglyme and cooled to −30 °C. A solution of $SbCl_3$ (0.49 g, 2.2 mmol) in 50 mL of tetraglyme was prepared in a nitrogen-filled glovebox and then placed in an addition funnel. The addition and workup procedures of this reaction were identical to that described above for method C, except that the volatiles produced during the reaction were continuously passed through traps held at −20 and −196 °C. The −196 °C trap was found to contain deuterostibine (0.19 g, 1.7 mmol, 77%). The −20 °C trap was employed to condense any tetraglyme, but at the reaction temperature of −30 °C, none was observed.

Vapor-phase FTIR of SbD_3: 2721 cm^{-1} (vw), 2683 cm^{-1} (w), 2647 cm^{-1} (vw), 1399 cm^{-1} (s), 1356 cm^{-1} (vs), 1320 cm^{-1} (s), 1138 cm^{-1} (w), 602 cm^{-1} (m,sh), 590 cm^{-1} (s), 557 cm^{-1} (s).

Acknowledgment. The authors would like to thank Dr. Karl Olander of ATMI's NovaSource Division for his financial support and fruitful discussions related to this field of research.

CM980121M